CHINESE OPTICS LETTERS

Vol. 21, No. 9 | September 2023

High-power single-frequency fiber amplifiers: progress and challenge [Invited]

Can Li (李 灿)[1*], Yue Tao (陶 悦)[1], Man Jiang (姜 曼)[1], Pengfei Ma (马鹏飞)[1,2,3], Wei Liu (刘 伟)[1,2,3], Rongtao Su (粟荣涛)[1,2,3], Jiangming Xu (许将明)[1], Jinyong Leng (冷进勇)[1,2,3], and Pu Zhou (周 朴)[1**]

[1] College of Advanced Interdisciplinary Studies, National University of Defense Technology, Changsha 410073, China

[2] Nanhu Laser Laboratory, National University of Defense Technology, Changsha 410073, China

[3] Hunan Provincial Key Laboratory of High Energy Laser Technology, National University of Defense Technology, Changsha 410073, China

*Corresponding author: lc0616@163.com

**Corresponding author: zhoupu203@163.com

Received April 18, 2023 | Accepted June 9, 2023 | Posted Online August 14, 2023

Unlike conventional continuous-wave lasers with wide spectra, the amplification of single-frequency lasers in optical fibers is much more difficult owing to the ultra-high power spectral density induced nonlinear stimulated Brillouin scattering effect. Nevertheless, over the past two decades much effort has been devoted to improving the power scaling and performance of high-power single-frequency fiber amplifiers. These amplifiers are mostly driven by applications, such as high precision detection and metrology, and have benefited from the long coherence length, low noise, and excellent beam quality of this type of laser source. In this paper, we review the overall development of high-power single-frequency fiber amplifiers by focusing on its progress and challenges, specifically, the strategies for circumventing the stimulated Brillouin scattering and transverse mode instability effects that, at present, are the major limiting factors of the power scaling of the single-frequency fiber amplifiers. These factors are also thoroughly discussed in terms of free-space and all-fiber coupled architecture. In addition, we also examine the noise properties of single-frequency fiber amplifiers, along with corresponding noise reducing schemes. Finally, we briefly envision the future development of high-power single-frequency fiber amplifiers.

Keywords: single frequency; fiber amplifier; stimulated Brillouin scattering; transverse mode instability; low noise.
DOI: 10.3788/COL202321.090002

1. Introduction

Single-frequency lasers are a kind of source that operates in a single-longitudinal-mode (SLM) regime of an optical oscillator. Thanks to their merits of long coherence length, low noise, and narrow spectral width, single-frequency lasers have found plenty of applications in, for example, high precision optical sensing, coherent communication, metrology, and spectroscopy[1–4]. Generally, single-frequency laser operation is realized from a laser cavity that has an oscillation mode spacing wide enough so that only a single oscillating mode can be retained with the aid of intra-cavity filtering components. The common practice is the employment of a short cavity length (several centimeters or even shorter), which incorporates a conventional narrowband filter that can realize stable SLM operation with a compact configuration[5]. At present, by using rare-earth ion-doped fibers, a solid-state crystal, or a semiconductor chip as the gain medium, single-frequency lasers with high performance output have been well-developed and even commercialized[6–8].

Nevertheless, for applications such as gravitational wave detection (GWD)[9], coherent lidar[10], and nonlinear frequency conversion[11], the power level of single-frequency laser sources that is directly output from a single oscillator is far from meeting the application requirements. For example, the Einstein Telescope (ET) was designed with a single-frequency laser power of 1 kW for the sake of decreasing the signal shot noise and increasing the sensitivity of GWD[12]. Regarding the amplification of the single-frequency laser, rare-earth ion-doped fibers are preferred as the gain medium, thanks to its peculiar waveguide structure, which has such advantages as a large surface area to volume ratio for heat dissipation, excellent thermo-optical properties, high conversion efficiency, and flexible manipulation. Over the past two decades, single-frequency fiber amplifiers (SFFAs) have continued to attract research interest concerning power scaling and performance improvement. However, a substantial review on this topic is still hard to find in the literature, except that in 2017 Ref. [13] briefly summarized

the progress of the power scaling of single frequency fiber lasers, and in the following year, Ref. [12] discussed the application of high-power SFFAs on GWD.

In this review, we examine the state-of-the-art progress of high power SFFAs operating in the continuous-wave (CW) regime, which has been the focus in recent years, while for the pulsed operation one can refer to Ref. [13]. Section 2 briefly discusses the general scheme of the SFFA and its limiting factors for power scaling. Section 3 covers the progress and challenge on the power scaling of the SFFA. In Section 4, we discuss the noise properties of the SFFA and its suppression techniques, as well as the strategies for realizing high-power low-noise single-frequency laser output. Finally, concluding remarks are given in Section 5.

2. Scheme of SFFA and Limitations for Power Scaling

2.1. Master oscillator power amplifier

The general scheme for the amplification of the single-frequency laser is the fiber master oscillator power amplifier (MOPA). The typical schematic configuration is shown in Fig. 1. The seed laser is first successively amplified by one or more pre-amplifiers before being launched into the main amplifier for power boosting. In common case, the main amplifier is forward pumped by N ($N \geq 2$) high-power multimode pump sources through an $(N+1)\times 1$ pump combiner. The amplified laser signal is then passed through a pump dump that is used to strip out the residual pump and multimode components, and then it is output to the free space via an endcap and a collimator. The main amplifier can also be backward pumped, i.e., the pump light transmits in reverse, or bidirectionally, with the laser signal. However, for the amplification of the single-frequency laser, owing to the detrimental fiber nonlinear effect (discussed in the next sub-section) that has a lower onset threshold at a longer transmission length, the forward pumping scheme that minimizes the transmitting length for the final amplified laser signal is the prime choice for power scaling. In addition, the configuration illustrated in Fig. 1 is in a compact all-fiber format, which is beneficial for the stable operation of the system and has a high tolerance to external perturbations. In contrast, in the case of using unconventional fibers, e.g., a large mode area (LMA) micro-structured photonic crystal fiber (PCF) as the gain medium of the main amplifier[14], fusion splicing it with existing fiber components becomes difficult. In this way, free-space coupling the pump and signal light into the gain fiber by leveraging bulky mirrors and lenses is commonly used, and only the system's compactness and robustness and the coupling efficiency of the pump and signal (the corresponding loss is ~2 dB) are sacrificed.

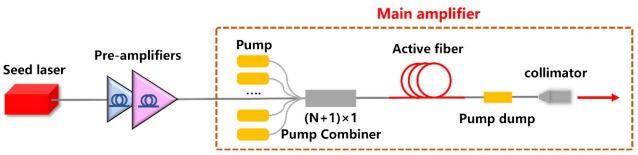

Fig. 1. Schematic configuration of a typical fiber MOPA system.

2.2. Stimulated Brillouin scattering (SBS) effect

With the LMA fiber-based MOPA scheme, the output power of the wide spectrum laser with a near diffraction-limited single-mode beam reached the 10-kW level in more than a decade ago[15]. However, the maximum output power of the SFFA still has not surpassed 1 kW, and the major limiting factor is the nonlinear SBS effect, which is a phenomenon where the laser signal is backwardly scattered by an acoustic wave that is induced by the process of electrostriction in the optical fiber, and which leads to the generation of Stokes light with a frequency downshift equal to the corresponding phonon frequency[16]. In general, the SBS threshold of a passive single mode fiber can be approximately evaluated by[17]

$$P_{\mathrm{th}} \cong 21\frac{KA_{\mathrm{eff}}}{g_B L_{\mathrm{eff}}}\left(1+\frac{\Delta\nu_l}{\Delta\nu_B}\right), \tag{1}$$

where K is the polarization factor of the laser signal, and it equals 1 and 2 for random and linear polarization, respectively. Otherwise, it is in between 1 and 2. A_{eff} and L_{eff} are the effective mode area and interaction length, respectively. g_B is the peak Brillouin gain, and it is intrinsically determined by the material and waveguide parameters of the fiber. Finally, $\Delta\nu_l$ and $\Delta\nu_B$ are the laser linewidth and Brillouin gain bandwidth (several tens of MHz), respectively. For the SFFA, the term in the parentheses of Eq. (1) is negligible since the linewidth of the single-frequency laser is generally less than 100 kHz.

The onset of SBS in a fiber MOPA system converts the amplified laser signal to the backward transmitted Stokes light and thus limits the achievable output power, as well as deteriorates the laser stability[18]. To suppress the SBS effect, the straightforward method is to increase the effective mode area and shorten the fiber length (i.e., using high gain fiber) of the main amplifier. To this end, the LMA fiber with a core diameter of up to 50 μm, while maintaining a low numeric aperture (NA) for single-mode light transmission, has been routinely employed to enhance the operation power of the SFFA[12,13]. As mentioned above, using the LMA fiber in the main amplifier would lead to the discarding of the monolithic fiber configuration and would complicate the system. This problem can be circumvented by leveraging the tapered fiber, which has a thin input end for fusion splicing with the pre-amplifier and a thick output end. In between the two ends, the core/cladding diameter is continuously enlarged for the suppression of the nonlinear effect and the enhancement of the pump absorption[19,20]. In addition, the gradually changed waveguide of the fiber would lead to a broadened SBS gain spectrum and decreased peak gain, resulting in a high SBS threshold and rendering the tapered fiber advantageous for constructing the all-fiber high power SFFA.

Considering the manipulation of the SBS gain, applying longitudinal temperature and strain gradients to the gain fiber also

proved to be efficient for introducing extra SBS frequency shifts and increasing the onset threshold[21–24]. For instance, we applied the strain gradient shown in Fig. 2(a) to a 2.5-m-long polarization-maintaining (PM) ytterbium-doped fiber (YDF) with a core/cladding diameter of 25/250 μm, and the corresponding simulated SBS gain spectrum manifests a significant broadening effect. The SBS gain peak is suppressed by around 4 times, as demonstrated in Fig. 2(b)[23]. In addition, the acoustical profile in the fiber can also be modified to efficiently suppress the SBS effect by tailoring the composition of the host material. For example, co-doping aluminum and germanium with an engineered fiber core profile has been demonstrated to effectively reduce the overlap, which is integral to the optical and acoustical fields[25,26].

It should be noted that Eq. (1) is a simplified version, on the precondition that the laser power of the laser signal is unchanged along the fiber, whereas in a practical amplifier, the laser power is significantly increased. In this case, the effective nonlinear length should be considered when estimating the SBS threshold. Specifically, in a counter-pumped SFFA, the pump power depletes quickly at the rare end of the gain fiber, and the signal power is boosted dramatically, while at the fore end, the powers of the laser signal and the pump are relatively low and therefore lead to an effectively shortened nonlinear interaction length and an increased SBS threshold. Moreover, along with the power evolution, the quantum defect induced heat deposition and thus the temperature also manifest remarkable variations along the longitudinal direction of the fiber, facilitating further suppression of the SBS effect[22,27]. Nevertheless, the scheme of the counter-pumping is generally demonstrated in a free-space coupling manner, since in the case of all-fiber coupling the amplified single-frequency laser would transmit in an extra segment of passive fiber in which the SBS process might be dominated[28]. Another method for leveraging the engineered power evolution of the amplifier to suppress the SBS effect is to introduce extra short wavelength laser components that consume a portion of the optical gain at the fore end of the gain fiber and convert to the laser signal at the rare end via the reabsorption effect. In this way, the induced significant variation of the signal power and the temperature along the fiber would effectively increase the SBS threshold[29–31]. However, this method is not commonly used since the system is prone to four-wave-mixing occurring under high power operation, although it can be implemented with an all-fiber forward-pumping manner.

2.3. Transverse mode instability effect

It is common sense that the LMA fiber is obligatory in realizing a high SBS threshold of SFFA. However, it inevitably brings in higher-order modes (HOMs) that would cause the so-called transverse mode instability (TMI), which deteriorates the laser stability and, more importantly, also impedes the power from increasing. In principle, HOMs interfere with the fundamental mode, and the generated model interference pattern (MIP) induces periodic refractive index grating (RIG) inside the fiber core via the thermal effects, leading to fast energy coupling between the HOMs and the fundamental mode when the operating power of the amplifier surpasses a certain threshold[32–34]. A characteristic behavior of TMI is the sudden degradation of the output beam quality and the distortion of the beam profile, as shown in Fig. 3. As such, although the very-large-mode-area (VLMA) fiber with a core diameter > 50 μm has been realized, it is mainly employed for the amplification of the energy of laser pulses with a low repetition rate; whereas for the average power scaling of single-frequency laser, the threshold of the thermally induced TMI tends to decrease with the enlarging of the fiber core diameter, demonstrating an opposite trend with that of the SBS effect[35,36]. Moreover, it is found that the laser linewidth significantly affects the TMI threshold, i.e., a narrower linewidth would result in a lower TMI threshold, manifesting a similar relationship between the linewidth and the SBS threshold in SFFAs[37,38].

At present, the TMI effect is one of the major obstacles to elevating the average output power of fiber lasers with diffraction-limited beam quality, and extensive research has been devoted to investigating its origin mechanism and mitigation methods[34,39]. Regarding the suppression of the TMI effect, the straightforward strategy is to decrease the HOM content inside the gain fiber, which generally has a mode field area large enough for suppressing the nonlinear effects such as SBS. In principle, to maintain the single transverse mode profile, the numerical aperture (NA) of the fiber should be decreased linearly with the increase of the core diameter, while the refractive

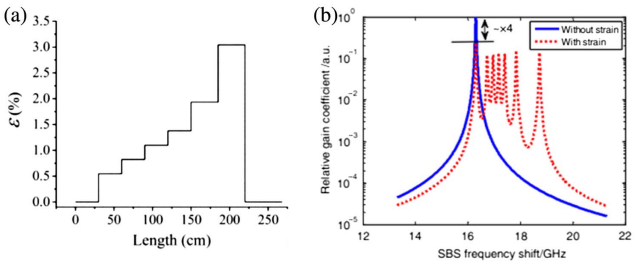

Fig. 2. (a) Applied strain distribution along the gain fiber. (b) Calculated effective SBS gain spectra with and without strain[23].

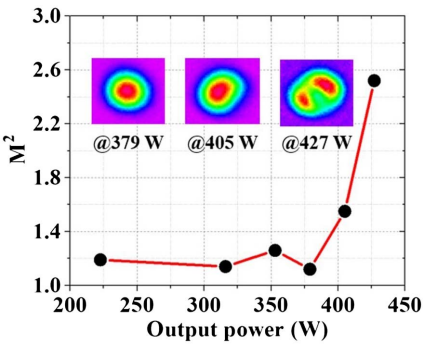

Fig. 3. Beam quality (M^2 factor) versus the output power of a typical SFFA. Insets: beam profiles at selected output powers[35].

index difference between the core and cladding of the fiber should be quadratically reduced. For a step-index fiber, due to the limitation of the tolerance control, the conventional manufacturing process generally can realize a small NA of 0.06, corresponding to a core diameter of 30 μm that can maintain single-mode light transmission[40]. In recent years, with the development of advanced fabricating techniques, the NA of the LMA fiber has been reduced to 0.02 with a core diameter of 50 μm[41,42]. Nevertheless, those ultra-low NA fibers with significantly increased core diameters generally have a low absorption coefficient at the same time and are incapable of absorbing sufficient pump power within a short length, which is mandatory for suppressing the SBS effect in the amplification of the single-frequency laser. The alternative method is to introduce considerable loss to the HOMs inside the fiber through engineering the cladding structure or refractive index profile. Many designs have been proposed and actualized, e.g., the well-known PCF[43], all-solid photonic bandgap fiber[44], the leakage channel fiber[45], the chirally coupled-core (3C) fiber[46], and large pitch fiber[36], to name a few. In addition, other than the fiber design, the HOM content can also be simply manipulated through bending the fiber with an appropriate radius.

However, the current situation is that nearly all of the high average power lasers with decent beam quality output have been obtained from fibers with core diameters less than 30 μm; whereas LMA fibers with thicker cores are generally employed to boost the energy of pulsed lasers, in which case the heat deposition during the amplification process is less severe[47–49]. To alleviate the thermal effect, which is directly responsible for the occurring of TMI, the most effective method is to decrease the quantum defect during laser amplification by reducing the interval between the pump and signal wavelengths. A typical scheme is the well-known tandem pumping, which has enabled the operation of YDF amplifiers with multi-kW output power at 1.0 μm with a 1018 nm pump[50–52]. However, owing to the small absorption cross section of the YDF at 1018 nm, a length of ~30 m is generally required to absorb enough pump power under the clad-pumping scheme, which is impracticable for increasing the power of single-frequency lasers. Exploiting the core pumping scheme can circumvent this problem and allow for the absorption of sufficient pump power with a YDF length that is short enough for SBS suppression. Nevertheless, limited by the available power of the single-mode 1018-nm laser and coupling optics, the maximum output power of a tandem core-pumped SFFA is currently limited at 252 W[53,54]. Another method that is effective in relieving the thermal issue is to develop LMA-YDFs that are immune, to a certain extent, to the photodarkening effect, which is responsible for the excess loss of the laser power and the heating of the fiber[55,56]. Although such fibers have not been utilized in constructing SFFAs yet, it should be helpful in the future for reliable emitting of high-power single-frequency lasers from a YDF with a large enough mode area.

In addition to suppressing the HOM content and thermal effect in LMA-YDF, the formation of RIG, as well as its phase shift with regards to the MIP, can also be manipulated to increase the TMI threshold. For instance, operating the amplifier in the saturation regime would weaken the strength of the RIG and suppress the TMI[39,57]. Moreover, the RIG was also demonstrated to be weakened by actively adding a dynamically switched π phase shift to the MIP with a high enough switching rate such that the RIG cannot efficiently mimic the changing MIP and then experiences a washing out effect[58]. As the implementation of this method currently requires spatially adjusting the coupling position of the laser signal on the input end of the main amplifier with bulky components, it is therefore not applicable to an all-fiber system. Another method that adopts the concept of washing out the RIG is modulating the pump power electrically with appropriate frequency and depth, for the sake of quickly modifying the periodicity of the MIP by intentionally changing the effective refractive index difference between the transverse modes with pump modulation-induced temperature profile variation[59]. However, as the modulation signal would be inevitably transferred to the amplified laser, this method is less attractive for SFFAs, which are widely known to generate highly stable and low-noise single-frequency lasers other than just the power scaling. In recent years, it was found that the low frequency pump power variation is responsible for producing the phase shift between the MIP and the RIG, as well as inducing the TMI under specific RIG strength[60,61].

More recent research has identified that the laser intensity noise is the main driving force for the TMI in high-power fiber amplifiers, and an experimental investigation has demonstrated that increasing the relative intensity noise (RIN) of the pump and the seed by ~3% (by imprinting white noise on the RIN spectrum from 1 Hz to 2 kHz) would decrease the TMI threshold by 63% and 13%, respectively, as shown in Fig. 4[62]. The reason why the pump noise has more significant influence on the TMI threshold than the seed noise might be attributed to the fact that a fiber amplifier generally behaves as a low-/high-pass filter to the pump/seed modulation[63]. As such, it is an intuitive

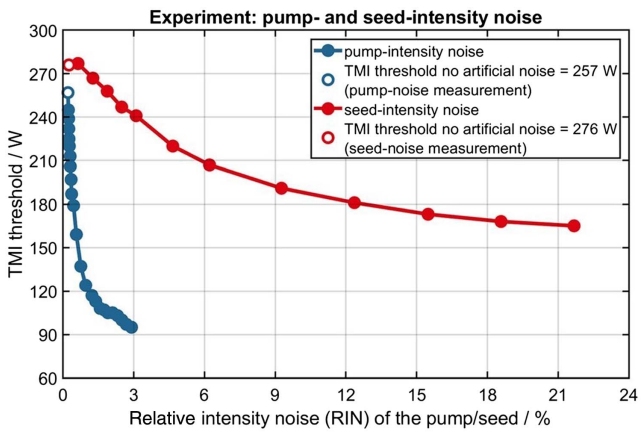

Fig. 4. TMI threshold as a function of the relative intensity noise (RIN) of the pump and the seed. The artificially imprinted noise contains frequencies from 1 Hz up to 2 kHz. The impact of the pump intensity noise (blue dots) on the TMI threshold is significantly stronger than that of the seed intensity noise (red dots)[61].

conclusion that an effective suppression of the TMI could be realized by reducing the low frequency RIN of the amplified laser, which is in fact, to some degree, an innate task for SFFAs that are mainly used for high-precision detection.

3. Progress and Challenges in Power Scaling SFFAs

3.1. Free-space coupling

Up to now, the major progress in the power scaling of SFFAs has been obtained at 1.0 μm, 1.5 μm, and 2.0 μm, and mostly endowed by the well-developed ytterbium-, erbium- and thulium-doped fiber (YDF, EDF, and TDF), as well as the corresponding pump sources and fiber components[5,13]. In addition, owing to the merits of a high pump absorption coefficient and low quantum defect (around 8%) of the YDF, it is more advantageous for scaling the output power of SFFAs than EDF and TDF. As far back as 2007, researchers respectively achieved more than 400 W linearly polarized and 500 W randomly polarized output power at 1.0 μm from SFFAs with LMA-YDF, while the SBS suppression was realized by engineering the overlap of the optical and acoustical fields or leveraging the temperature gradient induced SBS gain broadening[64,65]. Those power records had not been broken until 2014, when the TMI effect had already been found to be the major limiting factor for power scaling in LMA fiber amplifiers[66]. In Ref. [66], a dedicated, designed acoustic- and gain-tailored PM-LMA-YDF was employed to simultaneously suppress the SBS and TMI effect in the SFFA, and a maximum output power of 811 W was obtained. Further power enhancement was limited by the SBS effect, although the thermal gradient was also exploited to increase the SBS threshold. In 2015, an all-solid photonic bandgap YDF with a core diameter of ~50 μm and with specific dopants that are favorable to decreasing the Brillouin gain was employed to amplify the single-frequency laser, while the obtained output power was just 400 W, beyond which the TMI effect would emerge despite the estimated SBS threshold being more than 1 kW[67]. Later, in 2022, this fiber was further optimized for TMI suppression, which was realized by introducing multiple cladding resonance design to the fiber for restraining the HOM content, and the output power of the corresponding SFFA was increased to 500 W[68]. It is worth noting that all the aforementioned research is based on free-space coupling the signal and pump into the main amplifier, owing to the fact that the utilized LMA-YDFs are hardly incompatible with the all-fiber architecture. Although the free-space coupled configuration sacrifices the compact and reliable operation of the system, it allows for counter-pumping of the SFFA, enabling effective suppression of the SBS and the realization of the impressive high output power[64–68].

As for the EDF, owing to the relatively low erbium absorption cross sections and low doping concentrations in the silica fiber, ytterbium co-doping is routinely employed to obtain the well-known EYDF, which leverages the ytterbium to erbium energy transfer for efficient pump absorption[69]. In 2005, a 1.5 μm SFFA that adopted free-space counter-pumping of an LMA-EYDF had been demonstrated to produce 151 W single-frequency laser power, while further power increasing was hindered by the parasitic lasing at around 1.0 μm, owing to the excessive population inversion of the ytterbium that resulted from a larger pumping rate than the energy transfer rate[70]. A higher output power of 207 W was realized in 2015, and the trick was to pump the amplifier at the wavelength of 940 nm, at which the pump absorption is more than 4 times lower than at the absorption peak wavelength (976 nm) of the EYDF[71]. In this way, a longer active fiber is mandatory for efficient amplification, leading to a reduced ytterbium population inversion per unit length and suppressed 1.0 μm emission. It is noted here that the main amplifier in Ref. [71] was demonstrated with an all-fiber configuration, and the reason why we discuss it in this sub-section is that the corresponding result stands for the highest output power of the SFFA at 1.5 μm, while the involved scheme would be helpful for further increasing the power for a free-space coupled system.

Another limiting factor of the EYDF-based SFFA is the serious thermal issue that arises from its significant quantum defect, which is nearly ~40%[72,73]. To address this problem, tandem pumping the amplifier at ~1480 nm with Raman fiber amplifiers or erbium-doped fiber amplifiers (EDFAs) at ~1530 nm would be helpful, although currently the achievable output power is limited by the available pump power[74,75]. In addition, it is noted that the SBS is currently not the major restriction for the power scaling of 1.5 μm SFFAs, with which the TMI effect has not even been experimentally observed.

Regarding the TDF based SFFAs, thanks to the cross-relaxation effect of the thulium ions, which converts one pump photon at ~790 nm to two signal photons at 2.0 μm[76,77], it is more efficient than the 1.5 μm counterparts. In 2009, an output power as high as 608 W of a single-frequency laser at 2040 nm was achieved from a bidirectionally pumped LMA-TDF amplifier, with which a higher power can be obtained, given that more pump power is available[78]. Since the Brillouin gain is wavelength related and would decrease with the increasing wavelength[79], the nonlinear SBS effect is less serious for the amplification of single-frequency laser with a TDF as compared especially with a YDF, given that the corresponding mode field areas are commensurate. Nevertheless, a high power TDF amplifier still suffers from the thermal issue, as even under a perfect condition the quantum defect is still ~20% (over two times higher than that of the YDF amplifier) when pumped with the low cost and high brightness of a 790-nm pump. In fact, it is a consensus that even when pumped with a sufficient 790 nm laser, it is still challenging for a TDF amplifier to deliver more than 1 kW average power due to the serious heating effect[78]. Although the tandem pumping scheme with a ~1900 nm laser can alleviate the heat loads, the accordingly reduced absorption cross section requires a longer TDF length, which may bring in the issue of SBS when boosting the power of a single-frequency laser[80–82]. Fortunately, it has been verified theoretically[83] and experimentally[84] that the higher heat loads in the TDF amplifier do not lead to a lower TMI threshold, as

compared to the YDF amplifier. Actually, thanks to the wavelength dependent phase shift between the MIP and RIG (scales as λ^{-1}) and the cross-relaxation effect, which induced higher degrees of population saturation, the TMI threshold is considerably higher than expected such that it has, until recently, been first experimentally observed in a TDF amplifier[84].

3.2. All-fiber coupling

The previous sub-section shows that the record output powers of SFFAs at 1.0 μm, 1.5 μm, and 2.0 μm, respectively, have remained for nearly a decade. There is little research literature concerning the power scaling of free-spaced coupled SFFAs since the reporting of those records. On the contrary, in recent years, there has been continuous progress in increasing the output power of all-fiber SFFAs, especially at 1.0 μm and 2.0 μm, as demonstrated by the power evolution in Fig. 5, which is an updated version of Fig. 7 in Ref. [13]. Specifically, the light red zone basically represents the progress summarized in Ref. [13] in 2016, while the light green zone stands for the progress thereafter. Since the transmission length of the laser signal is longer for an all-fiber layout, and the utilized LMA fiber generally has a core diameter within 30 μm for fusion splicing, the SBS threshold of an all-fiber SFFA is considerably lower than that of a free-space coupled version. The situation is particularly representative at 1.0 μm, at which the power evolution of the SFFA shown in Fig. 5 can be regarded as the achievements of the SBS suppression until the year of 2020. For instance, in using a 2.8 m PM-LMA-YDF, which has a core/cladding diameter of 30/250 μm, we obtained a 332 W linearly polarized single-frequency laser with the measured beam quality (M^2 factor) of 1.4 in 2013[85]. Then in 2016, we utilized a PM-LMA-YDF with 25-μm-core diameter, with the assistance of a strain gradient applied along the fiber for SBS suppression, and a single-frequency laser power of 414 W was realized with a measured M^2 of 1.34[23].

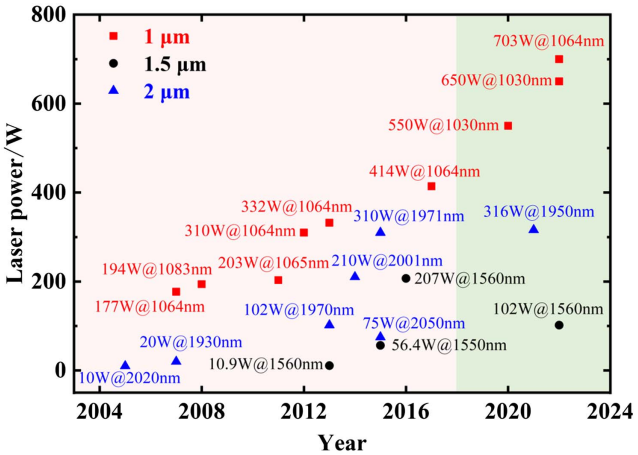

Fig. 5. Output power evolution of the CW single-frequency amplifiers in an all-fiber format operating in 1 μm, 1.5 μm, and 2 μm regions (an updated version of Fig. 7 in Ref. [13]).

After 2016, researchers began to try LMA-YDFs with a larger core size to amplify the 1.0 μm single-frequency laser with an all-fiber format, which then entered the phase of dealing with the TMI effect. In 2020, we used a tapered YDF with a core/cladding diameter of 36.1/249.3 μm at the thin end and 57.8/397.3 μm at the thick end to construct the main amplifier. We observed a TMI threshold of ~300 W while the SBS threshold was theoretically estimated to be over 2000 W[86]. To mitigate the TMI effect, we afterward shifted the operation wavelength of the system to 1030 nm, at which the thermal effect will be less serious owing to a decreased quantum defect, and a TMI-limited 379 W of single-polarization output was obtained with the configuration shown in Fig. 6. In addition, by manipulating the polarization state of the laser launched into the main amplifier, a 550 W output power of a non-polarized single-frequency laser with a measured M^2 of 1.47 was achieved[35]. In 2022, a 3C-YDF with a core diameter of 34 μm was employed to construct a counter-pumped all-fiber SFFA, with the combiner being integrated directly on the gain fiber[87]. Thanks to the HOM content suppression capability of the 3C fiber, a linearly polarized output power of 336 W with a fundamental mode content of over 90% was obtained, and further increasing the power was impeded by the onset of SBS.

In the same year, we used a confine-doped active fiber to construct a high power SFFA with the doping diameter of ~30 μm inside and an LMA core with a diameter of more than 40 μm. Since the proportion of HOMs in the amplified laser beam was considerably suppressed, increasing TMI threshold to more than 1.6 times obtained an SBS-limited single-frequency output power of 322 W with an M^2 factor of 1.25/1.33[88]. Subsequently, a further optimized confine-doped LMA-YDF associated with the longitudinal temperature gradient was adopted for amplifying the single-frequency laser to an output power of 386 W with an M^2 factor of 1.19/1.26[89].

Another recent work about mitigating the TMI effect in a high-power SFFA used leveraging of cascaded LMA-YDFs with different dopant concentrations and lengths for optimizing the heat loads, and hybrid pumping wavelengths (915 nm and 976 nm) with a delicately allocated power ratio for increasing the TMI threshold via a reinforced saturation level, with which a non-polarized single-frequency power of 435 W was obtained from a forward-pumped monolithic fiber amplifier with a core diameter of 30 μm[90]. By further optimizing the amplification system, the same group significantly pushed the output power to an impressive level of 703 W, with a spectral linewidth of

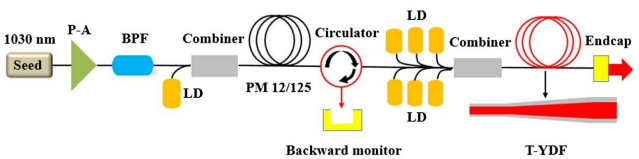

Fig. 6. Experimental setup of the tapered YDF-based SFFA at 1030 nm. P-A, pre-amplifier; BPF, bandpass filter; LD, laser diode; PM, polarization maintaining; YDF, Yb-doped fiber[35].

2 kHz and a measured M^2 of 1.4[91]. More recently, by associating the hybrid wavelength pumping and the tapered YDF, which has structural parameters similar to those in Ref. [86], researchers have realized a 650 W single-frequency and single-polarization laser output from an all-fiber amplifier, though there was a compromised M^2 factor of 1.7 and a polarization extinction ratio of 14 dB, which are disadvantageous for practical applications that generally involve high precision interference of the laser beam[92].

In the 2.0 μm spectral region, it is worth noting that none of the collected works in the light red zone of Fig. 5 have encountered the restriction of the SBS or TMI, while the claimed major limiting factor for further power increasing is the available 793 nm pump power, which is not that readily obtainable as the 915/976 nm pump. In 2015, we reached a milestone on the high-power all-fiber SFFA based on TDF, we realized a 310 W output power by forward-pumping an LMA-TDF with a core diameter of 25 μm, and no sign of SBS or saturation was observed[93]. After that, another development that achieved an output power of 316 W was made in 2021, and the main amplifier was constructed by using a PM-TDF with a core/cladding diameter of 20/300 μm, which resulted in a polarization extinction ratio of >17 dB and an M^2 factor of <1.2. However, the relatively smaller core size caused the system to be limited by the SBS effect when further increasing the pump power[94]. For the 1.5 μm band, the summarization in the light red zone of Fig. 5 is incomplete, as it should include the results of the 207 W output power obtained in Ref. [70] that were published in the year of 2015, which record, unfortunately, has not yet been surpassed. Nevertheless, there were demonstrations concerning power scaling associated with performance improvement of the SFFA[95–98].

4. Noise Performances of SFFAs

With the continuous power scaling of SFFAs, its application breadth and depth are mainly determined by the intensity and frequency noise performances, which, for instance, have been mandatorily required to be low enough for applications in GWD, laser cooling, and trapping of atoms[12,99]. Nevertheless, the noise properties, as well as its suppression of high power SFFAs, especially with power exceeding 100 W, are less investigated as compared with those of the single-frequency seed lasers, of which the intensity and frequency noise have been suppressed to near the shot-noise limit[100–102]. In the process of power amplification, the noise characteristics of the single-frequency laser will be unavoidably deteriorated mostly because of the unstable multi-mode pump, thermal and nonlinear effects, as well as ambient perturbations, such as air convection and mechanical vibration[103–105]. In addition, for SFFAs that employ LMA fibers, which generally support few HOMs, the HOMs would interfere with the fundamental mode under high power operation and induce the so-called beam pointing noise[12,106]. Although this effect is trivial and the amplifier is operated below the TMI threshold, the generated beam jitter of the laser signal is also detrimental for most applications. In addition, externally removing the HOMs with a mode cleaner cannot address it completely, since the pointing noise would be transferred into the intensity noise of the fundamental mode[107,108]. In view of this, a more desirable solution is to suppress the content of the HOMs by using, for example, an LMA fiber with a smaller core, given that the relatively compromised output power can meet the application requirements. In the following section, we mainly focus on the discussion of the intensity and frequency noise of SFFAs at the precondition that the detrimental SBS and TMI effects are not taking place.

4.1. Intensity noise

Essentially, the intensity noise of SFFAs is primarily transferred from that of the seed and pump power fluctuations, which modulate the dynamical gain of the amplifier and thus the power of the amplified signal. A pioneering theoretical analysis of the noise transferring process was first carried out in Ref. [109], in which the transfer functions of the seed and pump noise to the output power variation of a telecom fiber amplifier were analytically derived based on the rate equations and power transfer functions. In principle, the intrinsic mechanism of the noise transfer is the dynamic interaction of the pump or seed modulation with the population inversion of the gain fiber. Generally, the variation of the upper-level population and thus the laser gain adapts to that of the pump power, while it changes inversely with that of the seed power, i.e., under a certain pumping rate an increased signal power would lead to less optical gain and vice versa. In addition, the response of the fiber amplifier to the seed or the pump modulation has a finite bandwidth, beyond which the gain cannot follow the corresponding changes. From this perspective, the transfer function of a fiber amplifier to the seed and the pump modulation can be regarded as damped high-pass and low-pass filters, respectively, with an identical corner frequency owing to the same underlying physical process. According to the theoretical model developed in Ref. [109], the corner frequency of the high and low pass filtering processes can be written as

$$\omega_{\text{eff}} = P_s^0(L)B_s + P_p^0(L)B_p + 1/\tau. \tag{2}$$

Here, $P_s^0(L)$ and $P_p^0(L)$, respectively, denote the average power of the laser signal and pump at the end of the amplifier; B_s and B_p are respectively the coupling factors of the signal and the pump light in the active fiber; and τ is the fluorescence lifetime. In addition, based on the theoretical model, an example of the transfer functions for pump and seed power modulations is shown in Fig. 7[110]. It can be seen from the figure that below the corner frequency the intensity noise of the seed is considerably suppressed, while that of the pump source is almost retained. As the transfer functions are basically unchanged in the low frequency range, Ref. [111] simplified its analytical expressions at the zero-frequency under the precondition that the amplified signal power is much higher than the spontaneous emission and residual pump power as follows:

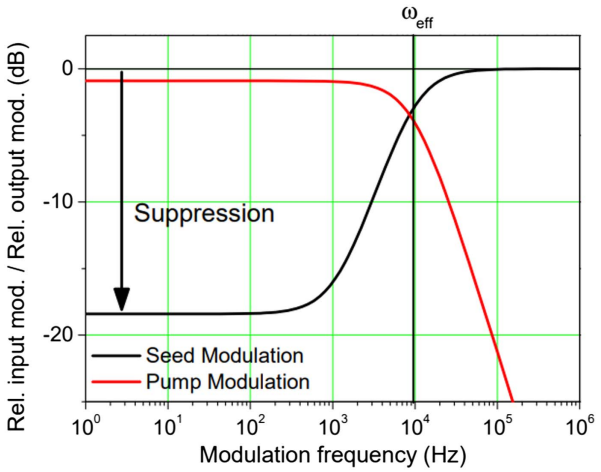

Fig. 7. Example of a transfer function for the pump and seed power modulation[110].

$$T_s = (P_s^0(0) + 1/(\tau B_s) + P_p^0(L)B_p/B_s)/P_s^0(L), \tag{3}$$

$$T_p = 1 - P_s^0(0)/P_s^0(L) + N_2/(\tau P_s^0(L)), \tag{4}$$

where T_s and T_p are, respectively, the transfer function of the seed and the pump; $P_s^0(0)$ is the input signal power; and N_2 is the population of the upper laser level. By using Eqs. (3) and (4), the intensity noise transfer properties in the low frequency range can be roughly estimated based on the input and output signal powers.

In addition, the low- and high-pass filtering effects of the fiber amplifier on the intensity noise of the pump and seed also offer guidelines for optimizing the noise performances of SFFAs. Specifically, it has been experimentally found that the pump power, the operating wavelength, and the absorption coefficient of the gain fiber affect the noise transfer processes of the SFFA apparently, with the association of the accordingly produced amplified spontaneous emission (ASE) effect, which is in fact not included in the above-mentioned theoretical model[111]. At present, the intensity noise of the single-frequency seed lasers has been well suppressed to near the shot-noise limit through the electrical or optical feedback methods[100–102], while those of the pump sources, especially the commonly employed high-power multi-mode laser diodes, are considerably high[112]. Moreover, a high power SFFA is generally configured in a multi-stage format, and the intensity noise of the laser signal would accordingly experience multi-stages of transferring. Therefore, even though a single-frequency seed laser with excellent noise performance is utilized, the seed intensity noise of the main amplifier is dominated by the pump of the last pre-amplifier, while the overall noise level of the amplified laser signal in the frequency range of interest is mostly determined by the pump noise of the main amplifier[113]. As such, a straightforward scheme to suppress the intensity noise of an SFFA is used to leverage the opto-electronic feedback loop to control the driving current of the pump at the last stage[114]. Nevertheless, it has been verified that the saturation effect of the fiber amplifier on the low frequency intensity noise of the seed laser can be compensated by modulating the signal power with engineered gain in the frequency domain, leading to the possibility of significantly suppressing the intensity noise of amplified laser through feedback controlling the seeding power. In 2017, an acoustic-optical modulator (AOM) was employed to adjust the seed power of a two-stage SFFA with an electronical feedback loop, and the intensity noise of the amplified signal at an output power of 2.5 W was suppressed in the frequency range of 10 Hz–100 kHz with a maximum reduction of 30 dB[112]. Subsequently, the same group exploited the electronical feedback method to control the pump driving current at the last stage of the SFFAs and realized a relative intensity noise (RIN) of −160 dBc/Hz at 3–20 kHz with output power of 100 W[115] and 2–10 kHz with output power of 365 W[116], respectively.

4.2. Frequency noise

In the process of fiber amplification, the degradation of the frequency noise of single-frequency lasers originates from the modulation of the fiber refractive index, which is mainly induced by the heat deposition from the upper laser level and the wavelength dependent gain via the Kramers–Kronig relation (KKR)[117]. As the latter is related to the nonlinear refractive index, which is very small for glass, its effect on the laser frequency noise can be neglected. In addition, there are currently no substantial models concerning the frequency noise transfer process in SFFAs. Previous research mainly focuses on experimentally measuring the laser phase noise that is produced during the amplification process by implementing a fiber interferometer that incorporates the fiber amplifier, as shown in Fig. 8[114,118]. The measurement results indicate that the excess phase/frequency noise is mainly dominated by the pump power noise-induced thermal fluctuations and the ambient temperature fluctuations in the low frequency range. Although it is trivial compared with that of the seed laser, in some high precision detection applications such as GWD, it still needs to be suppressed. Reference [114] has experimentally verified that

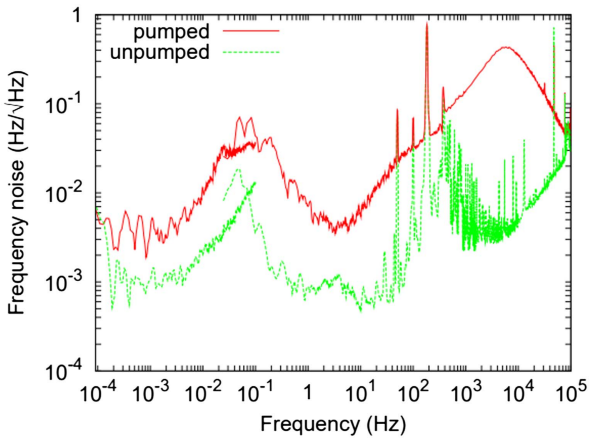

Fig. 8. Phase-noise measurements of the fiber amplifier scaled as frequency noise[114].

actively controlling the frequency of the seed laser with a piezoelectric transducer (PZT) could effectively compensate for the frequency noise deterioration of SFFAs based on the corresponding transfer function, though up to now this scheme has not been carried out. In 2013, further research revealed that the excess phase/frequency noise contributed from an SFFA is independent of the amplification gain and laser linewidth. Essentially, the spectral purity of the laser signal can be well preserved even with a linewidth as narrow as 1 Hz, given that the low frequency technical noise components of the amplifier are not unusually high[118]. Another noise component that arises from an SFFA is the ASE, which would be prominent especially under a high pumping rate, a low seeder power, or a small emission cross section of the gain fiber at the signal wavelength[119,120]. In terms of the effect of ASE on the laser frequency noise, it has been reported that the generated ASE in the SFFA would add additive components to the amplified signal, and thus broaden the laser linewidth[121]. Nevertheless, this effect can be readily addressed in most cases by optimizing the design of the amplifier to suppress the generation of ASE.

4.3. Low noise amplification and coherent beam combining

For most applications of high-power single-frequency lasers, low noise operation is mandatory, especially for high precision sensing and metrology. Although it is inevitable that the noise properties of an SFFA would degrade compared with those of the single-frequency seed laser, there are still efforts concerning the development of low-noise SFFAs that meet the requirements of specific applications by optimizing the amplifier design without the cumbersome opto-electronic feedback scheme. For instance, it has been demonstrated that, given that the detrimental SBS and ASE effects are insignificant, the integrated RIN of an Yb-doped SFFA from 1 kHz to 10 MHz can be as low as 0.012% at an output power of 50 W, by optimizing the current driver noise of the pump, the seeder power, the active fiber length, and the optical feedback of the fiber end[122]. In addition, employing a seeder laser with a very low level of noise could also lead to improved noise performance of the amplified single-frequency laser, and this has been respectively verified at 1.0 μm[123], 1.5 μm[95], and 2.0 μm[124], respectively. With the routine optimizing strategy, there have been demonstrations on low-noise Yb-doped SFFAs that operate at the edge range of the Yb emission with the output power of several tens of watts, aiming to provide interrogating sources for such applications as atomic spectroscopy[125–127]. In addition, low-noise SFFAs with higher operation powers (maximum 200 W) have also been reported at 1.0 μm[107,108] and 1.5 μm[96], respectively, for applications in the well-known GWD. Our other research demonstrated the tandem core-pumping of an all-fiber SFFA that adopts YDF with core/cladding diameter of 20/130 μm as the gain medium, which delivered a maximum output power of more than 250 W with excellent beam quality[54]. As with the pumping of a single-mode 1018-nm fiber laser, the low frequency intensity noise of the amplified laser under maximal power was measured to be comparable to that of the single-frequency seed laser and was considerably lower than that of the pre-amplifier, which was pumped by multi-mode laser diodes at 976 nm. Recently, researchers have demonstrated that by optimizing the signal and pump power, the length of the active fiber, and the pumping manner of the SFFA, a saturated even-distribution gain along the active fiber can be realized, resulting in an apparent suppression of the RIN in the seed laser while the power is boosted.[128]. Nevertheless, in this work the SFFA was operated in the sub-watt regime, and the feasibility of the corresponding noise suppression scheme is yet to be verified with much higher output power.

At present, the output power level of low-noise SFFAs lags behind the corresponding record power, mostly because the thermal and nonlinear effects, as well as the ASE, would become significant at higher operation power. Therefore, realizing higher output power of SFFAs with desired noise performance remains the main topic for researchers. For instance, the next-generation gravitational wave detector might be designed with a single-frequency laser power as high as 1 kW, which leads to a considerably decreased shot-noise level of the source and would further increase the detection sensitivity[12]. Adopting the active feedback control scheme has been verified to be effective in suppressing the low frequency intensity noise of high-power SFFAs, while its effect on other laser properties, such as the frequency noise, linewidth, and polarization degree, are yet to be examined[115,116]. Another effective method for obtaining a high power low-noise single-frequency laser source is to coherently combine the output of two or more SFFAs that operate at a relatively low power with a decent noise performance. In fact, back in 2011, we reported the coherent combining of nine SFFAs with an output power of 120 W, and a final combined power of more than 1 kW was achieved through phase locking of the tiled amplifier array[129]. However, in this proof-of-concept experiment, the noise properties of the laser were not characterized. In the same year, Ref. [130] demonstrated the coherent combining of two SFFAs with an output power of 10 W in a filled-aperture manner and proved that the noise performance, as well as the beam quality of a single-fiber amplifier, can be well reserved after the combination. In 2016, Ref. [131] further reported the coherent combining of two 40 W SFFAs, and the measured overall performance of the combined beam satisfies the requirements for GWD with the Advanced Virgo detector. In terms of higher operation power, as at present the maximum reported output power of a low-noise SFFA without active control is around 200 W[107], researchers reproduced four SFFAs based on the same structure design and verified a good repetitiveness of the noise properties as well as other laser performance. This indicated that a much higher power of high-performance single-frequency laser source is achievable through coherent combining of the high power SFFAs[132]. This was subsequently demonstrated in Ref. [133], in which filled-aperture coherent beam combining was implemented with two 200 W SFFAs and a combined power of 398 W was obtained, with comparable noise performance to that of the single fiber amplifiers in terms of power fluctuation (shown in Fig. 9), beam pointing, and frequency jitter.

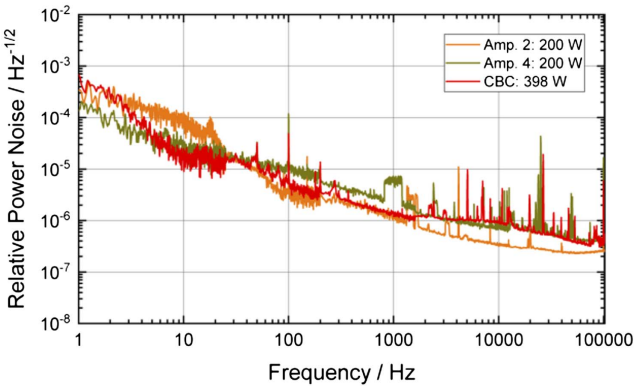

Fig. 9. Relative power noise of the combined beam in comparison with the single amplifier performance. Relative power noise variations are caused by the amplifier pumps[133].

5. Conclusion

In this paper, we have reviewed the progress of SFFAs in terms of power scaling and noise reduction and discussed the corresponding technical challenges. Essentially, the record output power of a single SFFA has reached 800 W at 1.0 μm, and it has remained there for nearly a decade. The major limiting factors are the nonlinear SBS and thermally induced TMI effects, of which the suppressing scheme conflicts with each other. In addition, in recent years, many research efforts have been focused on increasing the output power of SFFAs using an all-fiber format, which imposes a much lower SBS threshold to the system because it employs a smaller fiber core and a larger fiber length for splicing and connecting. With the development of the tapered fiber, this issue has been largely circumvented, and the output powers of all-fiber SFFAs have reached similar levels of output power in free-space coupled counterparts. At present, the association of the SBS and the TMI effects has also become the main restriction to the power increasing of all-fiber SFFAs. Further power scaling requires an overall consideration of both the effects and the proposed optimum design of the active fiber and the amplifier architecture[134,135].

The noise performance of the SFFAs is intrinsically critical for most of their applications, while it was paid less attention in the early stages of their development, when the active LMA-PCF with free-space configuration was commonly adopted to obtain high-power output. With the rapid development of all-fiber SFFAs in recent years, low-noise single-frequency lasers with several hundreds of watts output power have been realized by employing opto-electronic feedback control and optimizing the fiber and amplifier design, as well as by employing coherent combining of multiple low-power amplifiers. In fact, the all-fiber architecture represents an integrated monolithic system that is more robust and immune to external disturbances, as well as advantageous for obtaining a high-power output beam with excellent quality and pointing noise, which are also important for applications concerning coherent detection. It is noted that an enabling technology of the all-fiber SFFA is the fabrication of components that can be fusion spliced with the active LMA fibers, for the sake of coupling the signal and pump sources into the last stage amplifier. With the continuous development of the fabrication techniques of the fiber components, in the future more specially designed LMA fibers would be exploited to demonstrate all-fiber SFFAs with higher output power and further improved performance[136-138]. In addition, as it has been verified that the laser intensity noise is a driver for the onset of the TMI effect, and an improved noise performance can lead to a higher TMI threshold[139], it is expectable that though suppressing the low frequency noise of the amplifier, a much higher power of the single-frequency laser with a lower noise level would be achievable, while avoiding the dilemma of mitigating the TMI and the SBS effects simultaneously. Moreover, this dilemma can be also avoided by exploiting the scheme of coherent beam combining, while also compromising the system's compactness and the laser performance, such as noise, polarization, and beam quality, needing further characterization and optimization. Other than power scaling and performance improving, another research direction of the SFFA is to extend the operation wavelength range to meet the application needs, as most of the previous research was carried out at 1.0 μm. For instance, the LIGO Voyager has been designed with a high-power low-noise single-frequency laser source at 2.0 μm to reduce the thermal noise of the mirror coating and to realize a substantial increasement of the GWD sensitivity[140]. Moreover, for applications such as metrology and atomic spectroscopy that employ high-power and high-performance single-frequency lasers in the visible band, SFFAs with tailored operation wavelengths are routinely required to generate those sources through nonlinear frequency conversion[141-143].

Acknowledgement

This work was supported by the National Key R&D Program of China (No. 2020YFC2200401) and the National Natural Science Foundation of China (Nos. 62005316 and 62035015).

References

1. B. P. Abbott, *et al.* (LIGO Scientific Collaboration and Virgo Collaboration), "Observation of gravitational waves from a binary black hole merger," Phys. Rev. Lett. **116**, 061102 (2016).
2. S. Okamoto, M. Terayama, M. Yoshida, K. Kasai, T. Hirooka, and M. Nakazawa, "Experimental and numerical comparison of probabilistically shaped 4096 QAM and a uniformly shaped 1024 QAM in all-Raman amplified 160 km transmission," Opt. Express **26**, 3535 (2018).
3. E. Oelker, R. B. Hutson, C. J. Kennedy, L. Sonderhouse, T. Bothwell, A. Goban, D. Kedar, C. Sanner, J. M. Robinson, G. E. Marti, D. G. Matei, T. Legero, M. Giunta, R. Holzwarth, F. Riehle, U. Sterr, and J. Ye, "Demonstration of 4.8×10^{-17} stability at 1 s for two independent optical clocks," Nat. Photonics **13**, 714 (2019).
4. T. Wu, X. Peng, W. Gong, Y. Zhan, Z. Lin, B. Luo, and H. Guo, "Observation and optimization of ^{4}He atomic polarization spectroscopy," Opt. Lett. **38**, 986 (2013).
5. Z. Yang, C. Li, S. Xu, and C. Yang, *Single-Frequency Fiber Lasers* (Springer, 2019).
6. http://www.npphotonics.com/single-frequency-lasers.
7. http://www.rio-lasers.com/_products/1064 mn-orion.
8. https://www.coherent.com/lasers/main/mephisto-lasers.

9. D. Castelvecchi, "Gravitational-wave observatory LIGO set to double its detecting power," Nature **566**, 305 (2019).
10. K. Wang, C. Gao, Z. Lin, Q. Wang, M. Gao, S. Huang, and C. Chen, "1645 nm coherent Doppler wind lidar with a single-frequency Er:YAG laser," Opt. Express **28**, 14694 (2020).
11. M. K. Shukla and R. Das, "High-power single-frequency source in the mid-infrared using a singly resonant optical parametric oscillator pumped by Yb-fiber laser," IEEE J. Sel. Top. Quantum Electron. **24**, 5100206 (2017).
12. M. Steinke, H. Tünnermann, V. Kuhn, T. Theeg, M. Karow, O. Varona, P. Jahn, P. Booker, J. Neumann, P. Weßels, and D. Kracht, "Single-frequency fiber amplifiers for next-generation gravitational wave detectors," IEEE J. Sel. Top. Quantum Electron. **24**, 3100613 (2018).
13. S. Fu, W. Shi, Y. Feng, L. Zhang, Z. Yang, S. Xu, X. Zhu, R. A. Norwood, and N. Peyghambarian, "Review of recent progress on single-frequency fiber lasers [Invited]," J. Opt. Soc. Am. B **34**, A49 (2017).
14. M. Hildebrandt, M. Frede, P. Kwee, B. Willke, and D. Kracht, "Single-frequency master-oscillator photonic crystal fiber amplifier with 148 W output power," Opt. Express **14**, 11071 (2006).
15. M. O'Connor, V. Gapontsev, V. Fomin, M. Abramov, and A. Ferin, "Power scaling of SM fiber lasers toward 10 kW," in *Lasers and Electro-Optics/International Quantum Electronics Conference*, OSA Technical Digest (Optica, 2009), paper CThA3.
16. A. Kobyakov, M. Sauer, and D. Chowdhury, "Stimulated Brillouin scattering in optical fibers," Adv. Opt. Photon. **2**, 1 (2010).
17. T. Shimizu, K. Nakajima, K. Shiraki, K. Ieda, and I. Sankawa, "Evaluation methods and requirements for the stimulated Brillouin scattering threshold in a single-mode fiber," Opt. Fiber Technol. **14**, 10 (2008).
18. X. Guan, C. Yang, P. Ma, Q. Zhao, Z. Zhang, W. Lin, X. Wei, Z. Yang, and S. Xu, "Influence of stimulated Brillouin scattering on the noise evolution of high-power all-fiber single-frequency MOPA system," Opt. Laser Technol. **128**, 106212 (2020).
19. V. Filippov, Y. K. Chamorovskii, K. M. Golant, A. Vorotynskii, and O. G. Okhotnikov, "Optical amplifiers and lasers based on tapered fiber geometry for power and energy scaling with low signal distortion," Proc. SPIE **9728**, 97280V (2016).
20. K. Bobkov, A. Levchenko, T. Kashaykina, S. Aleshkina, M. Bubnov, D. Lipatov, A. Laptev, A. Guryanov, Y. Leventoux, G. Granger, V. Couderc, S. Février, and M. Likhachev, "Scaling of average power in sub-MW peak power Yb-doped tapered fiber picosecond pulse amplifiers," Opt. Express **29**, 1722 (2021).
21. M. Hildebrandt, S. Büsche, P. Weßels, M. Frede, and D. Kracht, "Brillouin scattering spectra in high-power single-frequency ytterbium doped fiber amplifiers," Opt. Express **16**, 15970 (2008).
22. A. Liu, X. Chen, M.-J. Li, J. Wang, D. T. Walton, and L. A. Zenteno, "Comprehensive modeling of single frequency fiber amplifiers for mitigating stimulated Brillouin scattering," J. Lightwave Technol. **27**, 2189 (2009).
23. L. Huang, H. Wu, R. Li, L. Li, P. Ma, X. Wang, J. Leng, and P. Zhou, "414 W near-diffraction-limited all-fiberized single-frequency polarization-maintained fiber amplifier," Opt. Lett. **42**, 1 (2017).
24. Z. Lou, K. Han, X. Wang, H. Zhang, and X. Xu, "Increasing the SBS threshold by applying a flexible temperature modulation technique with temperature measurement of the fiber core," Opt. Express **28**, 13323 (2020).
25. A. Kobyakov, S. Kumar, D. Q. Chowdhury, A. Boh Ruffin, M. Sauer, S. R. Bickham, and R. Mishra, "Design concept for optical fibers with enhanced SBS threshold," Opt. Express **13**, 5338 (2005).
26. M. Li, X. Chen, J. Wang, S. Gray, A. Liu, J. A. Demeritt, A. Boh Ruffin, A. M. Crowley, D. T. Walton, and L. A. Zenteno, "Al/Ge co-doped large mode area fiber with high SBS threshold," Opt. Express **15**, 8290 (2007).
27. Y. Jeong, J. Nilsson, J. K. Sahu, D. N. Payne, R. Horley, L. M. B. Hickey, and P. W. Turner, "Power scaling of single-frequency Ytterbium-doped fiber master-oscillator power-amplifier sources up to 500 W," IEEE J. Sel. Top. Quantum Electron. **13**, 546 (2007).
28. A. Liu, "Stimulated Brillouin scattering in single-frequency fiber amplifiers with delivery fibers," Opt. Express **17**, 15201 (2009).
29. I. Dajani, C. Zeringue, C. Lu, C. Vergien, L. Henry, and C. Robin, "Stimulated Brillouin scattering suppression through laser gain competition: scalability to high power," Opt. Lett. **35**, 3114 (2010).
30. C. Zeringue, C. Vergien, and I. Dajani, "Pump-limited, 203 W, single-frequency monolithic fiber amplifier based on laser gain competition," Opt. Lett. **36**, 618 (2011).
31. L. J. Henry, T. M. Shay, D. W. Hult, and K. B. Rowland, "Thermal effects in narrow linewidth single and two tone fiber lasers," Opt. Express **19**, 6164 (2011).
32. T. Eidam, C. Wirth, C. Jauregui, F. Stutzki, F. Jansen, H.-J. Otto, O. Schmidt, T. Schreiber, J. Limpert, and A. Tünnermann, "Experimental observations of the threshold-like onset of mode instabilities in high power fiber amplifiers," Opt. Express **19**, 13218 (2011).
33. H.-J. Otto, F. Stutzki, F. Jansen, T. Eidam, C. Jauregui, J. Limpert, and A. Tünnermann, "Temporal dynamics of mode instabilities in high-power fiber lasers and amplifiers," Opt. Express **20**, 15710 (2012).
34. C. Jauregui, C. Stihler, and J. Limpert, "Transverse mode instability," Adv. Opt. Photon. **12**, 429 (2020).
35. W. Lai, P. Ma, W. Liu, L. Huang, C. Li, Y. Ma, and P. Zhou, "550 W single frequency fiber amplifiers emitting at 1030 μm based on a tapered Yb-doped fiber," Opt. Express **28**, 20908 (2020).
36. F. Stutzki, F. Jansen, H.-J. Otto, C. Jauregui, J. Limpert, and A. Tünnermann, "Designing advanced very-large-mode-area fibers for power scaling of fiber-laser systems," Optica **1**, 233 (2014).
37. M. Kuznetsov, O. Vershinin, V. Tyrtyshnyy, and O. Antipov, "Low-threshold mode instability in Yb^{3+}-doped few-mode fiber amplifiers," Opt. Express **22**, 29714 (2014).
38. M. N. Zervas, "Transverse-modal-instability gain in high power fiber amplifiers: effect of the perturbation relative phase," APL Photon. **4**, 022802 (2019).
39. R. Tao, X. Wang, and P. Zhou, "Comprehensive theoretical study of mode instability in high-power fiber lasers by employing a universal model and its implications," IEEE J. Sel. Top. Quantum Electron. **24**, 0903319 (2018).
40. M.-J. Li, X. Chen, A. Liu, S. Gray, J. Wang, D. T. Walton, and L. A. Zenteno, "Limit of effective area for single-mode operation in step-index large mode area laser fibers," J. Lightwave Technol. **27**, 3010 (2009).
41. F. Kong, C. Dunn, J. Parsons, M. T. Kalichevsky-Dong, T. W. Hawkins, M. Jones, and L. Dong, "Large-mode-area fibers operating near single-mode regime," Opt. Express **24**, 10295 (2016).
42. W. Xu, Z. Lin, M. Wang, S. Feng, L. Zhang, Q. Zhou, D. Chen, L. Zhang, S. Wang, C. Yu, and L. Hu, "50 μm core diameter $Yb^{3+}/Al^{3+}/F^{-}$ codoped silica fiber with $M^2 < 1.1$ beam quality," Opt. Lett. **41**, 504 (2016).
43. J. Limpert, O. Schmidt, J. Rothhardt, F. Röser, T. Schreiber, A. Tünnermann, S. Ermeneux, P. Yvernault, and F. Salin, "Extended single-mode photonic crystal fiber lasers," Opt. Express **14**, 2715 (2006).
44. L. Dong, F. Kong, G. Gu, T. W. Hawkins, M. Jones, J. Parsons, M. T. Kalichevsky-Dong, K. Saitoh, B. Pulford, and I. Dajani, "Large-mode-area all-solid photonic bandgap fibers for the mitigation of optical nonlinearities," IEEE J. Sel. Top. Quantum Electron. **22**, 4900207 (2016).
45. L. Dong, H. A. McKay, L. Fu, M. Ohta, A. Marcinkevicius, S. Suzuki, and M. E. Fermann, "Ytterbium-doped all glass leakage channel fibers with highly fluorine-doped silica pump cladding," Opt. Express **17**, 8962 (2009).
46. X. Ma, C. Zhu, I.-N. Hu, A. Kaplan, and A. Galvanauskas, "Single-mode chirally coupled-core fibers with larger than 50 μm diameter cores," Opt. Express **22**, 9206 (2014).
47. Q. Chu, Q. Shu, Y. Liu, R. Tao, D. Yan, H. Lin, J. Wang, and F. Jing, "3 kW high OSNR 1030 nm single-mode monolithic fiber amplifier with a 180 pm linewidth," Opt. Lett. **45**, 6502 (2020).
48. P. Ma, H. Xiao, W. Liu, H. Zhang, X. Wang, J. Leng, and P. Zhou, "All-fiberized and narrow-linewidth 5 kW power-level fiber amplifier based on a bidirectional pumping configuration," High Power Laser Sci. Eng. **9**, e45 (2021).
49. E. Shestaev, D. Hoff, A. M. Sayler, A. Klenke, S. Hädrich, F. Just, T. Eidam, P. Jójárt, Z. Várallyay, K. Osvay, G. G. Paulus, A. Tünnermann, and J. Limpert, "High-power ytterbium-doped fiber laser delivering few-cycle, carrier-envelope phase-stable 100 μJ pulses at 100 kHz," Opt. Lett. **45**, 97 (2020).
50. P. Zhou, H. Xiao, J. Leng, J. Xu, Z. Chen, H. Zhang, and Z. Liu, "High-power fiber lasers based on tandem pumping," J. Opt. Soc. Am. B **34**, A29 (2017).
51. P. Ma, H. Xiao, D. Meng, W. Liu, R. Tao, J. Leng, Y. Ma, R. Su, P. Zhou, and Z. Liu, "High power all-fiberized and narrow-bandwidth MOPA system by tandem pumping strategy for thermally induced mode instability suppression," High Power Laser Sci. Eng. **6**, e57 (2018).
52. Z. Wang, W. Yu, J. Tian, T. Qi, D. Li, Q. Xiao, P. Yan, and M. Gong, "5.1 kW tandem-pumped fiber amplifier seeded by random fiber laser with high

suppression of stimulated Raman scattering," J. Quantum Electron. **57**, 6800109 (2021).
53. T. Theeg, C. Ottenhues, H. Sayinc, J. Neumann, and D. Kracht, "Core-pumped single-frequency fiber amplifier with an output power of 158 W," Opt. Lett. **41**, 9 (2016).
54. Y. Tao, M. Jiang, L. Liu, C. Li, P. Zhou, and Z. Jiang, "Over 250 W low noise core-pumped single-frequency all-fiber amplifier," Opt. Express **31**, 10586 (2023).
55. N. Zhao, W. Li, J. Li, G. Zhou, and J. Li, "Elimination of the photodarkening effect in an Yb-doped fiber laser with deuterium," J. Lightwave Technol. **37**, 3021 (2019).
56. N. Zhao, K. Peng, J. Li, Y. Chu, G. Zhou, and J. Li, "Photodarkening effect suppression in Yb-doped fiber through the nanoporous glass phase-separation fabrication method," Opt. Mat. Express **9**, 1085 (2019).
57. L. Huang, R. Tao, C. Shi, D. Meng, H. Zhang, P. Ma, X. Wang, and P. Zhou, "Towards the enhancement of the TMI threshold in monolithic high-power fiber system by controlling the pump distribution and the seed power," IEEE Photon. J. **10**, 1504312 (2018).
58. H.-J. Otto, C. Jauregui, F. Stutzki, F. Jansen, J. Limpert, and A. Tünnermann, "Controlling mode instabilities by dynamic mode excitation with an acousto-optic deflector," Opt. Express **21**, 17285 (2013).
59. C. Jauregui, C. Stihler, A. Tünnermann, and J. Limpert, "Pump-modulation-induced beam stabilization in high-power fiber laser systems above the mode instability threshold," Opt. Express **26**, 10691 (2018).
60. C. Stihler, C. Jauregui, A. Tünnermann, and J. Limpert, "Phase-shift evolution of the thermally induced refractive index grating in high-power fiber laser systems induced by pump-power variations," Opt. Express **26**, 19489 (2018).
61. C. Stihler, C. Jauregui, A. Tünnermann, and J. Limpert, "Modal energy transfer by thermally induced refractive index gratings in Yb-doped fibers," Light Sci. Appl. **7**, 59 (2018).
62. C. Stihler, C. Jauregui, S. E. Kholaif, and J. Limpert, "Intensity noise as a driver for transverse mode instability in fiber amplifiers," PhotoniX **1**, 8 (2020).
63. S. Novak and A. Moesle, Analytic model for gain modulation in EDFAs, J. Lightwave Technol. **20**, 975 (2002).
64. Y. Jeong, J. Nilsson, J. K. Sahu, D. N. Payne, R. Horley, L. M. B. Hickey, and P. W. Turner, "Power scaling of single-frequency ytterbium-doped fiber master-oscillator power-amplifier sources up to 500 W," IEEE J. Sel. Top. Quantum Electron. **13**, 546 (2007).
65. S. Gray, A. Liu, D. T. Walton, J. Wang, M.-J. Li, X. Chen, A. Boh Ruffin, J. A. DeMeritt, and L. A. Zenteno, "502 Watt, single transverse mode, narrow linewidth, bidirectionally pumped Yb-doped fiber amplifier," Opt. Express **15**, 17044 (2007).
66. C. Robin, I. Dajani, and B. Pulford, "Modal instability-suppressing, single-frequency photonic crystal fiber amplifier with 811 W output power," Opt. Lett. **39**, 666 (2014).
67. B. Pulford, T. Ehrenreich, R. Holten, F. Kong, T. W. Hawkins, L. Dong, and I. Dajani, "400-W near diffraction-limited single-frequency all-solid photonic bandgap fiber amplifier," Opt. Lett. **40**, 2297 (2015).
68. T. Matniyaz, S. P. Bingham, M. T. Kalichevsky-Dong, T. W. Hawkins, B. Pulford, and L. Dong, "High-power single-frequency single-mode all-solid photonic bandgap fiber laser with kHz linewidth," Opt. Lett. **47**, 377 (2022).
69. D. Y. Shen, J. K. Sahu, and W. A. Clarkson, "Highly efficient Er, Yb-doped fiber laser with 188 W free-running and > 100 W tunable output power," Opt. Express **13**, 4916 (2005).
70. Y. Jeong, J. K. Sahu, D. B. S. Soh, C. A. Codemard, and J. Nilsson, "High-power tunable single-frequency single-mode erbium: ytterbium codoped large-core fiber master-oscillator power amplifier source," Opt. Lett. **30**, 2997 (2005).
71. D. Creeden, H. Pretorius, J. Limongelli, and S. D. Setzler, "Single frequency 1560 nm Er:Yb fiber amplifier with 207 W output power and 50.5% slope efficiency," Proc. SPIE **9728**, 97282L (2016).
72. T. Matniyaz, F. Kong, M. T. Kalichevsky-Dong, and L. Dong, "302 W single-mode power from an Er/Yb fiber MOPA," Opt. Lett. **45**, 2910 (2020).
73. W. Yu, Q. Xiao, L. Wang, Y. Zhao, T. Qi, P. Yan, and M. Gong, "219.6 W large-mode-area Er:Yb codoped fiber amplifier operating at 1600 nm pumped by 1018 nm fiber lasers," Opt. Lett. **46**, 2192 (2021).
74. J. Feng, X. Cheng, H. Jiang, and Y. Feng, "45 W single frequency Er:Yb co-doped fiber amplifier at 1530 nm," Opt. Fiber Technol. **77**, 103282 (2023).
75. X. Cheng, Z. Lin, X. Yang, S. Cui, X. Zeng, H. Jiang, and Y. Feng, "High-power 1560 nm single-frequency erbium fiber amplifier core-pumped at 1480 nm," High Power Laser Sci. Eng. **10**, e3 (2022).
76. S. D. Jackson, A. Sabella, and D. G. Lancaster, "Application and development of high-power and highly efficient silica-based fiber lasers operating at 2 μm," IEEE J. Sel. Top. Quantum Electron. **13**, 567 (2007).
77. P. F. Moulton, G. A. Rines, E. V. Slobodtchikov, K. F. Wall, G. Frith, B. Samson, and A. L. G. Carter, "Tm-doped fiber lasers: fundamentals and power scaling," IEEE J. Sel. Top. Quantum Electron. **15**, 85 (2009).
78. G. D. Goodno, L. D. Book, and J. E. Rothenberg, "Low-phase-noise, single-frequency, single-mode 608 W thulium fiber amplifier," Opt. Lett. **34**, 1204 (2009).
79. M. Nikles, L. Thevenaz, and P. A. Robert, "Brillouin gain spectrum characterization in single-mode optical fibers," J. Lightwave Technol. **15**, 1842 (1997).
80. A. Sincore, J. D. Bradford, J. Cook, L. Shah, and M. C. Richardson, "High average power thulium-doped silica fiber lasers: review of systems and concepts," IEEE J. Sel. Top. Quantum Electron. **24**, 0901808 (2018).
81. D. Creeden, B. R. Johnson, G. A. Rines, and S. D. Setzler, "High power resonant pumping of Tm-doped fiber amplifiers in core- and cladding-pumped configurations," Opt. Express **22**, 29067 (2014).
82. Y. Wang, J. Yang, C. Huang, Y. Luo, S. Wang, Y. Tang, and J. Xu, "High power tandem-pumped thulium-doped fiber laser," Opt. Express **23**, 2991 (2015).
83. A. V. Smith and J. J. Smith, "Mode instability thresholds for Tm-doped fiber amplifiers pumped at 790 nm," Opt. Express **24**, 975 (2016).
84. C. Gaida, M. Gebhardt, T. Heuermann, Z. Wang, C. Jauregui, and J. Limpert, "Transverse mode instability and thermal effects in thulium-doped fiber amplifiers under high thermal loads," Opt. Express **29**, 14963 (2021).
85. P. Ma, P. Zhou, Y. Ma, R. Su, X. Xu, and Z. Liu, "Single-frequency 332 W, linearly polarized Yb-doped all-fiber amplifier with near diffraction-limited beam quality," Appl. Opt. **52**, 4854 (2013).
86. L. Huang, W. Lai, P. Ma, J. Wang, R. Su, Y. Ma, C. Li, D. Zhi, and P. Zhou, "Tapered Yb-doped fiber enabled monolithic high-power linearly polarized single-frequency laser," Opt. Lett. **45**, 4001 (2020).
87. S. Hochheim, E. Brockmüller, P. Wessels, J. Koponen, T. Lowder, S. Novotny, B. Willke, J. Neumann, and D. Kracht, "Single-frequency 336 W spliceless all-fiber amplifier based on a chirally coupled-core fiber for the next generation of gravitational wave detectors," J. Lightwave Technol. **40**, 2136 (2022).
88. W. Li, S. Ren, Y. Deng, Y. Chen, Y. Lu, W. Liu, P. Ma, Z. Pan, Z. Chen, L. Si, and P. Zhou, "Investigation of the confined-doped fiber on single-mode operating and power scaling in all-fiber single-frequency amplifiers," Front. Phys. **10**, 1016047 (2022).
89. W. Li, Z. Yan, S. Ren, Y. Deng, Y. Chen, P. Ma, W. Liu, L. Huang, Z. Pan, P. Zhou, and L. Si, "Confined-doped active fiber enabled all-fiber high-power single-frequency laser," Opt. Lett. **47**, 5024 (2022).
90. C. Shi, S. Fu, X. Deng, Q. Sheng, Y. Xu, Q. Fang, S. Sun, J. Zhang, W. Shi, and J. Yao, "435 W single-frequency all-fiber amplifier at 1064 nm based on cascaded hybrid active fibers," Opt. Commun. **502**, 127428 (2022).
91. C. Shi, X. Deng, S. Fu, Q. Sheng, P. Jiang, Z. Shi, Y. Li, W. Shi, and J. Yao, "700 W single-frequency all-fiber amplifier at 1064 nm with kHz-level spectral linewidth," Front. Phys. **10**, 982900 (2022).
92. W. Jiang, C. Yang, Q. Zhao, Q. Gu, J. Huang, K. Jiang, K. Zhou, Z. Feng, Z. Yang, and S. Xu, "650 W all-fiber single-frequency polarization-maintaining fiber amplifier based on hybrid wavelength pumping and tapered Yb-doped fibers," Photonics **9**, 518 (2022).
93. X. Wang, X. Jin, W. Wu, P. Zhou, X. Wang, H. Xiao, and Z. Liu, "310-W single frequency Tm-doped all-fiber MOPA," IEEE Photon. Technol. Lett. **27**, 677 (2015).
94. X. Guan, C. Yang, Q. Gu, W. Lin, T. Tan, Q. Zhao, X. Wei, Z. Yang, and S. Xu, "316 W high-brightness narrow-linewidth linearly polarized all-fiber single-frequency laser at 1950 nm," Appl. Phys. Express **14**, 112004 (2021).

95. C. Yang, X. Guan, Q. Zhao, B. Wu, Z. Feng, J. Gan, H. Cheng, M. Peng, Z. Yang, and S. Xu, "High-power and near-shot-noise-limited intensity noise all-fiber single-frequency 1.5 μm MOPA laser," Opt. Express **25**, 13324 (2017).
96. O. De Varona, W. Fittkau, P. Booker, T. Theeg, M. Steinke, D. Kracht, J. Neumann, and P. Wessels, "Single-frequency fiber amplifier at 1.5 μm with 100 W in the linearly polarized TEM_{00} mode for next-generation gravitational wave detectors," Opt. Express **25**, 24880 (2017).
97. X. Guan, Q. Zhao, W. Lin, T. Tan, C. Yang, P. Ma, Z. Yang, and S. Xu, "High-efficiency and high-power single-frequency fiber laser at 1.6 μm based on cascaded energy-transfer pumping," Photonics Res. **8**, 414 (2020).
98. J. Huang, Q. Zhao, J. Zheng, C. Huang, Q. Gu, W. Jiang, K. Zhou, C. Yang, Z. Feng, Q. Zhang, Z. Yang, and S. Xu, "A 102 W high-power linearly-polarized all-fiber single-frequency laser at 1560 nm," Photonics **9**, 396 (2022).
99. J. Hu, L. Zhang, H. Liu, K. Liu, Z. Xu, and Y. Feng, "High power room temperature 1014.8 nm Yb fiber amplifier and frequency quadrupling to 253.7 nm for laser cooling of mercury atoms," Opt. Express **21**, 30958 (2013).
100. C. Li, S. Xu, X. Huang, Y. Xiao, Z. Feng, C. Yang, K. Zhou, W. Lin, J. Gan, and Z. Yang, "All-optical frequency and intensity noise suppression of single-frequency fiber laser," Opt. Lett. **40**, 1964 (2015).
101. Q. Zhao, S. Xu, K. Zhou, C. Yang, C. Li, Z. Feng, M. Peng, H. Deng, and Z. Yang, "Broad-bandwidth near-shot-noise-limited intensity noise suppression of a single-frequency fiber laser," Opt. Lett. **41**, 1333 (2016).
102. Q. Zhao, K. Zhou, Z. Wu, C. Yang, Z. Feng, H. Cheng, J. Gan, M. Peng, Z. Yang, and S. Xu, "Near quantum-noise limited and absolute frequency stabilized 1083 nm single-frequency fiber laser," Opt. Lett. **43**, 42 (2018).
103. M. Tröbs, P. Weßels, and C. Fallnich, "Power- and frequency-noise characteristics of an Yb-doped fiber amplifier and actuators for stabilization," Opt. Express **13**, 2224 (2005).
104. C. Ye, L. Petit, J. J. Koponen, I.-N. Hu, and A. Galvanauskas, "Short-term and long-term stability in ytterbium-doped high-power fiber lasers and amplifiers," IEEE J. Sel. Top. Quantum Electron. **20**, 188 (2014).
105. X. Guan, C. Yang, P. Ma, Q. Zhao, Z. Zhang, W. Lin, X. Wei, Z. Yang, and S. Xu, "Influence of stimulated Brillouin scattering on the noise evolution of high-power all-fiber single-frequency MOPA system," Opt. Laser Technol. **128**, 106212 (2020).
106. P. Kwee, C. Bogan, K. Danzmann, M. Frede, H. Kim, P. King, J. Pöld, O. Puncken, R. L. Savage, F. Seifert, P. Wessels, L. Winkelmann, and B. Willke, "Stabilized high-power laser system for the gravitational wave detector advanced LIGO," Opt. Express **20**, 10617 (2012).
107. F. Wellmann, M. Steinke, F. Meylahn, N. Bode, B. Willke, L. Overmeyer, J. Neumann, and D. Kracht, "High power, single-frequency, monolithic fiber amplifier for the next generation of gravitational wave detectors," Opt. Express **27**, 28523 (2019).
108. A. Buikema, F. Jose, S. J. Augst, P. Fritschel, and N. Mavalvala, "Narrow-linewidth fiber amplifier for gravitational-wave detectors," Opt. Lett. **44**, 3833 (2019).
109. S. Novak and A. Moesle, "Analytic model for gain modulation in EDFAs," J. Lightwave Technol. **20**, 975 (2002).
110. H. Tünnermann, J. Neumann, D. Kracht, and P. Weßels, "Gain dynamics and refractive index changes in fiber amplifiers: a frequency domain approach," Opt. Express **20**, 13539 (2012).
111. L. Liu, C. Li, Y. Tao, M. Jiang, and P. Zhou, "Intensity noise transfer properties of a Yb-doped single-frequency fiber amplifier," Appl. Opt. **62**, 206 (2023).
112. J. Zhao, G. Guiraud, F. Floissat, B. Gouhier, S. Rota-Rodrigo, N. Traynor, and G. Santarelli, "Gain dynamics of clad-pumped Yb-fiber amplifier and intensity noise control," Opt. Express **25**, 357 (2017).
113. P. Gierschke, C. Jauregui, T. Gottschall, and J. Limpert, "Relative amplitude noise transfer function of an Yb^{3+}-doped fiber amplifier chain," Opt. Express **27**, 17041 (2019).
114. M. Tröbs, P. Wessels, and C. Fallnich, "Power- and frequency-noise characteristics of an Yb-doped fiber amplifier and actuators for stabilization," Opt. Express **13**, 2224 (2005).
115. J. Zhao, G. Guiraud, C. Pierre, F. Floissat, A. Casanova, A. Hreibi, W. Chaibi, N. Traynor, J. Boullet, and G. Santarelli, "High-power all-fiber ultra-low noise laser," Appl. Phys. B **124**, 114 (2018).
116. C. Dixneuf, G. Guiraud, Y.-V. Bardin, Q. Rosa, M. Goeppner, A. Hilico, C. Pierre, J. Boullet, N. Traynor, and G. Santarelli, "Ultra-low intensity noise, all fiber 365 W linearly polarized single frequency laser at 1064 nm," Opt. Express **28**, 10960 (2020).
117. M. Tröbs, P. Wessels, and C. Fallnich, "Phase-noise properties of an ytterbium-doped fiber amplifier for the laser interferometer space antenna," Opt. Lett. **30**, 789 (2005).
118. I. Ricciardi, S. Mosca, P. Maddaloni, L. Santamaria, M. De Rosa, and P. De Natale, "Phase noise analysis of a 10 Watt Yb-doped fibre amplifier seeded by a 1-Hz-linewidth laser," Opt. Express **21**, 14618 (2013).
119. B. Gouhier, G. Guiraud, S. Rota-Rodrigo, J. Zhao, N. Traynor, and G. Santarelli, "25 W single-frequency, low noise fiber MOPA at 1120 nm," Opt. Lett. **43**, 308 (2018).
120. D. Darwich, Y. Bardin, M. Goeppner, and C. Dixneuf, "Influence of pump properties on the tunability of 1.5 μm low-noise single frequency fiber amplifier," IEEE Photon. Technol. Lett. **34**, 27 (2021).
121. M. Xue, C. Gao, L. Niu, S. Zhu, and C. Sun, "Influence of amplified spontaneous emission on laser linewidth in a fiber amplifier," Appl. Opt. **59**, 2610 (2020).
122. G. Guiraud, N. Traynor, and G. Santarelli, "High-power and low-intensity noise laser at 1064 nm," Opt. Lett. **41**, 4040 (2016).
123. C. Yang, S. Xu, D. Chen, Y. Zhang, Q. Zhao, C. Li, K. Zhou, Z. Feng, J. Gan, and Z. Yang, "52 W kHz-linewidth low-noise linearly-polarized all-fiber single-frequency MOPA laser," J. Opt. **18**, 055801 (2016).
124. Q. Zhang, Y. Hou, X. Wang, W. Song, X. Chen, W. Bin, J. Li, C. Zhao, and P. Wang, "5 W ultra-low-noise 2 μm single-frequency fiber laser for next-generation gravitational wave detectors," Opt. Lett. **45**, 4911 (2020).
125. B. Gouhier, S. Rota-Rodrigo, G. Guiraud, N. Traynor, and G. Santarelli, "Low-noise single-frequency 50 W fiber laser operating at 1013 nm," Laser Phys. Lett. **16**, 045103 (2019).
126. B. Gouhier, C. Dixneuf, A. Hilico, G. Guiraud, N. Traynor, and G. Santarelli, "Low intensity noise high-power tunable fiber-based laser around 1007 nm," J. Lightwave Technol. **37**, 3539 (2019).
127. L. Liu, C. Li, Y. Tao, M. Jiang, P. Ma, and P. Zhou, "Over 30 W single-frequency all-fiber amplifier at 1120 nm with high ASE suppression," Appl. Opt. **62**, 1323 (2023).
128. C. Zeng, W. Peng, Q. Zhao, W. Lin, C. Yang, Y. Sun, C. Wang, Z. Feng, Z. Yang, and S. Xu, "Simultaneous achievement of power boost and low-frequency intensity noise suppression in a bidirectional pumping fiber amplifier based on saturated even-distribution gain," Opt. Express **31**, 5122 (2023).
129. Y. Ma, X. Wang, J. Leng, H. Xiao, X. Dong, J. Zhu, W. Du, P. Zhou, X. Xu, L. Si, Z. Liu, and Y. Zhao, "Coherent beam combination of 1.08 kW fiber amplifier array using single frequency dithering technique," Opt. Lett. **36**, 951 (2011).
130. H. Tünnermann, J. H. Pöld, J. Neumann, D. Kracht, B. Willke, and P. Weßels, "Beam quality and noise properties of coherently combined ytterbium doped single frequency fiber amplifiers," Opt. Express **19**, 19600 (2011).
131. L. Wei, F. Cleva, and C. N. Man, "Coherently combined master oscillator fiber power amplifiers for advanced Virgo," Opt. Lett. **41**, 5817 (2016).
132. F. Wellmann, M. Steinke, P. Wessels, N. Bode, F. Meylahn, B. Willke, L. Overmeyer, J. Neumann, and D. Kracht, "Performance study of a high-power single-frequency fiber amplifier architecture for gravitational wave detectors," Appl. Opt. **59**, 7945 (2020).
133. F. Wellmann, N. Bode, P. Wessels, L. Overmeyer, J. Neumann, B. Willke, and D. Kracht, "Low noise 400 W coherently combined single frequency laser beam for next generation gravitational wave detectors," Opt. Express **29**, 10140 (2021).
134. B. G. Ward, "Maximizing power output from continuous-wave single-frequency fiber amplifiers," Opt. Lett. **40**, 542 (2015).
135. J. T. Young, C. R. Menyuk, C. Wei, and J. Hu, "Increasing the power threshold in fiber amplifiers considering both the transverse mode and Brillouin instabilities," in *Conference on Lasers and Electro-Optics*, Technical Digest (Optica, 2022), paper SM2L.

136. D. Stachowiak, "High-power passive fiber components for all-fiber lasers and amplifiers application—design and fabrication," Photonics **5**, 38 (2018).
137. E. Brockmüller, F. Wellmann, D. Lutscher, O. Kimmelma, T. Lowder, S. Novotny, R. Lachmayer, J. Neumann, and D. Kracht, "CO_2-laser-ablation-assisted fabrication of signal-pump combiners with chirally coupled core fibers for co- and counter-pumped all-fiber amplifiers," Opt. Express **30**, 25946 (2022).
138. X. Chen, T. Yao, L. Huang, Y. An, H. Wu, Z. Pan, and P. Zhou, "Functional fibers and functional fiber-based components for high-power lasers," Adv. Fiber Mater. **5**, 59 (2023).
139. Q. Chu, C. Guo, X. Yang, F. Li, D. Yan, H. Zhang, and R. Tao, "Increasing mode instability threshold by mitigating driver noise in high power fiber amplifiers," IEEE Photon. Technol. Lett. **33**, 1515 (2021).
140. R. X. Adhikari, K. Arai, and A. F. Brooks, et al., "A cryogenic silicon interferometer for gravitational-wave detection," Class. Quantum Grav. **37**, 165003 (2020).
141. J. Dong, X. Zeng, S. Cui, J. Zhou, and Y. Feng, "More than 20 W fiber-based continuous-wave single frequency laser at 780 nm," Opt. Express **27**, 35362 (2019).
142. M.-D. Li, Y.-G. Zheng, W.-Y. Zhang, X.-K. Wang, B. Xiao, Z.-Y. Zhou, L. Jiang, M.-Z. Lian, Z.-S. Yuan, and J.-W. Pan, "A high-power and low-noise 532-nm continuous-wave laser for quantum gas microscopy," Rev. Sci. Instrum. **92**, 083202 (2021).
143. S. Cui, X. Zeng, H. Jiang, X. Cheng, X. Yang, J. Zhou, and Y. Feng, "Robust single-frequency 589 nm fiber laser based on phase modulation and passive demodulation," Opt. Express **30**, 9112 (2022).